eLIFE elifesciences.org

RESEARCH ARTICLE

Figures and figure supplements

Straightjacket/α2δ3 deregulation is associated with cardiac conduction defects in myotonic dystrophy type 1

Emilie Auxerre-Plantié *et al*

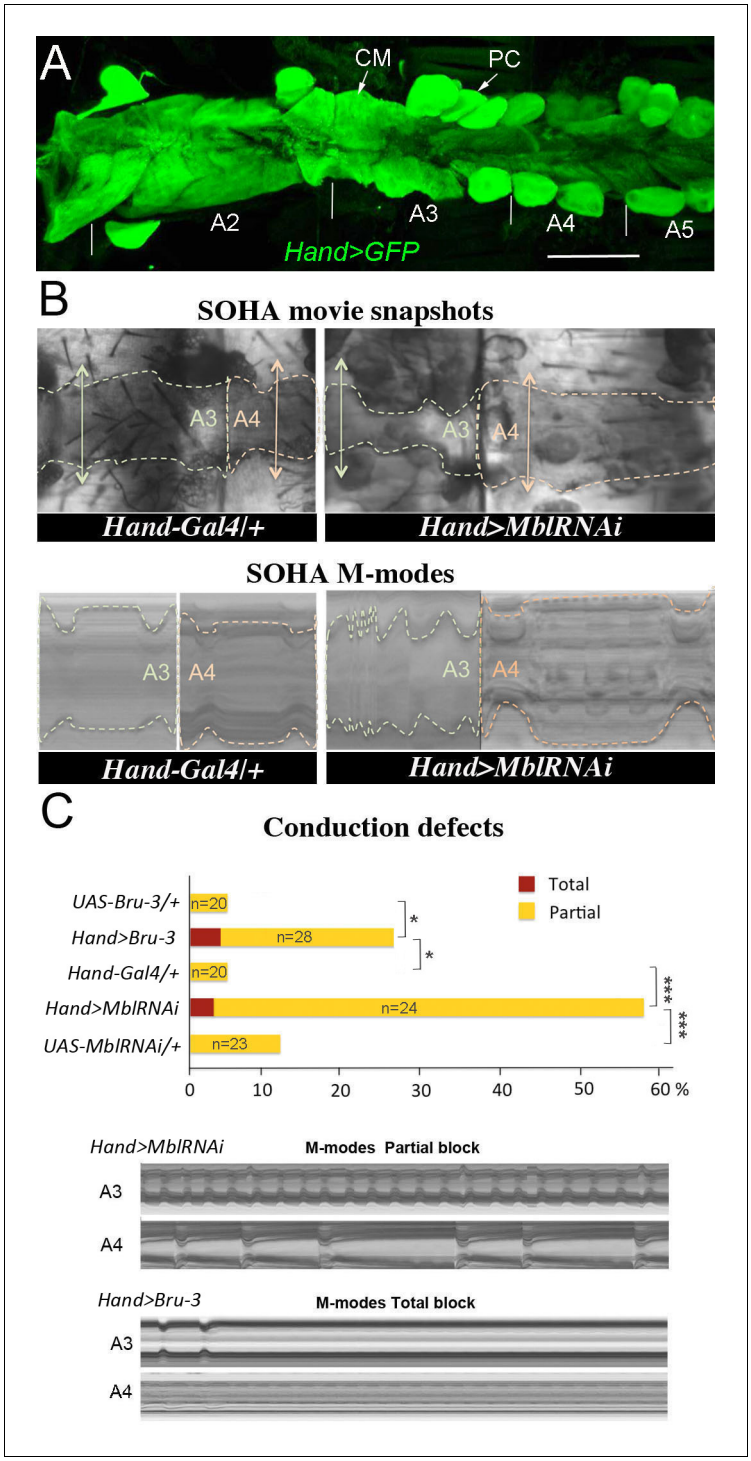

Figure 1. Cardiac-specific knockdown of MBNL1 ortholog and overexpression of CELF1 counterpart in *Drosophila* lead to asynchronous heartbeats. (**A**) The adult *Drosophila* heart expressing Hand-Gal4-driven GFP (*Hand>GFP*). Note that this Gal4 line drives expression exclusively in the heart. Arrows indicate cardiomyocytes (CM) and pericardial cells (PC) and A2–A5 denote abdominal segments. Scale bar, 150 µm. (**B**) Movie and M-modes views illustrating asynchronous heartbeats in *Hand>MblRNAi* flies registered in two adjacent heart segments (A3 and A4). Two-sided arrows indicate heart diameter in diastolic state. (**C**) Barplot graph showing percentage of flies with conduction defects in the different genetic contexts tested. Note the higher impact of attenuation of *Mbl* compared to overexpression of *Bru-3*. Number of fly hearts tested (n) is indicated and statistical significance (Fisher's exact test) denoted by * ($p<0.05$) and *** ($p<0.001$). Below are examples of M-modes illustrating 'partial' and 'total' heart blocks observed in *Hand>MblRNAi* and *Hand>Bru-3* flies developing conduction defects.

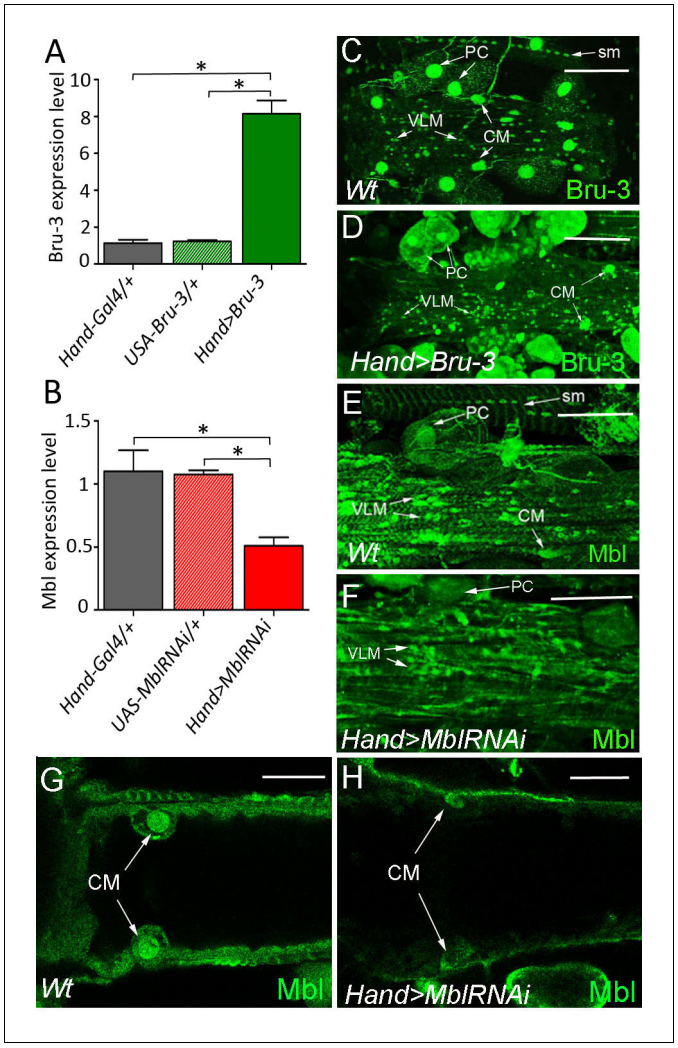

Figure 1—figure supplement 1. Bru-3 and Mbl are expressed in the adult fly heart and their transcript and protein levels are affected in *Hand*>Bru-*3* and *Hand>MblRNAi* flies. (**A–B**) RT-qPCR analyses of Bru-3 overexpression and Mbl attenuation in the adult hearts from *Hand>Bru-3* (**A**) and *Hand>MblRNAi* (**B**) flies. Three biological replicates (n = 10–12 hearts per replicate) were analysed for each condition. Statistical significance (Mann Whitney U test) is denoted by * ($p<0.05$) (**C–F**) Optical projection views of A3 cardiac segment showing expression of Bru-3 (**C–D**) and Mbl (**E–H**) proteins in the hearts of wild-type (*Wt*) (**C, E**), *Hand>Bru-3* (**D**) and *Hand>MblRNAi* (**F**) flies. (**G, H**) show confocal optical sections at the level of cardiomyocytes (CM) to document attenuation of Mbl in CMs nuclei. Bru-3 protein is detected in the nuclei of CMs, pericardial cells (PC) and ventral longitudinal muscle (VLM). A faint granular cytoplasmic expression could also be detected in PCs (**C**). Notice an increase of Bru-3 levels in *Hand>Bru-3* context (**D**) with more cytoplasmic Bru-3 signal detected in PCs and CMs. Similarly, Mbl accumulation is observed in CMs, PCs and the VLM nuclei (**E**). Apparent sarcomeric localization of Mbl is also detected in circular fibers of CMs and in the VLM (**E**). Notice Bru-3 and Mbl expression in nuclei of somatic muscles (sm). Scale bars (**C–F**) 100 µm; (**G,H**) 50 µm.

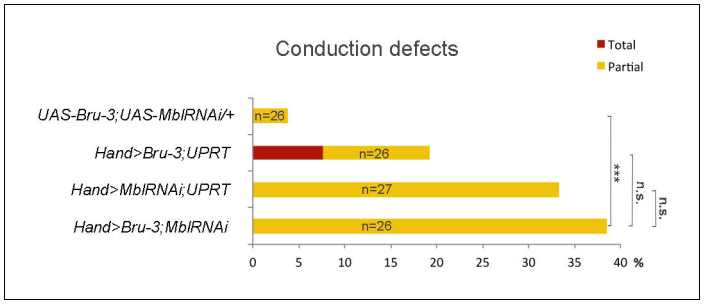

Figure 1—figure supplement 2. Effect of simultaneous cardiac attenuation of *Mbl* and overexpression of *Bru-3* on conduction defects. Barplot graph showing percentage of flies with conduction defects. Note a moderate additive effect of simultaneous attenuation of *Mbl* and overexpression of *Bru-3*. Number of fly hearts tested (n) is indicated and statistical significance (Fisher's exact test) denoted by ns ($p>0.05$) and *** ($p<0.001$).

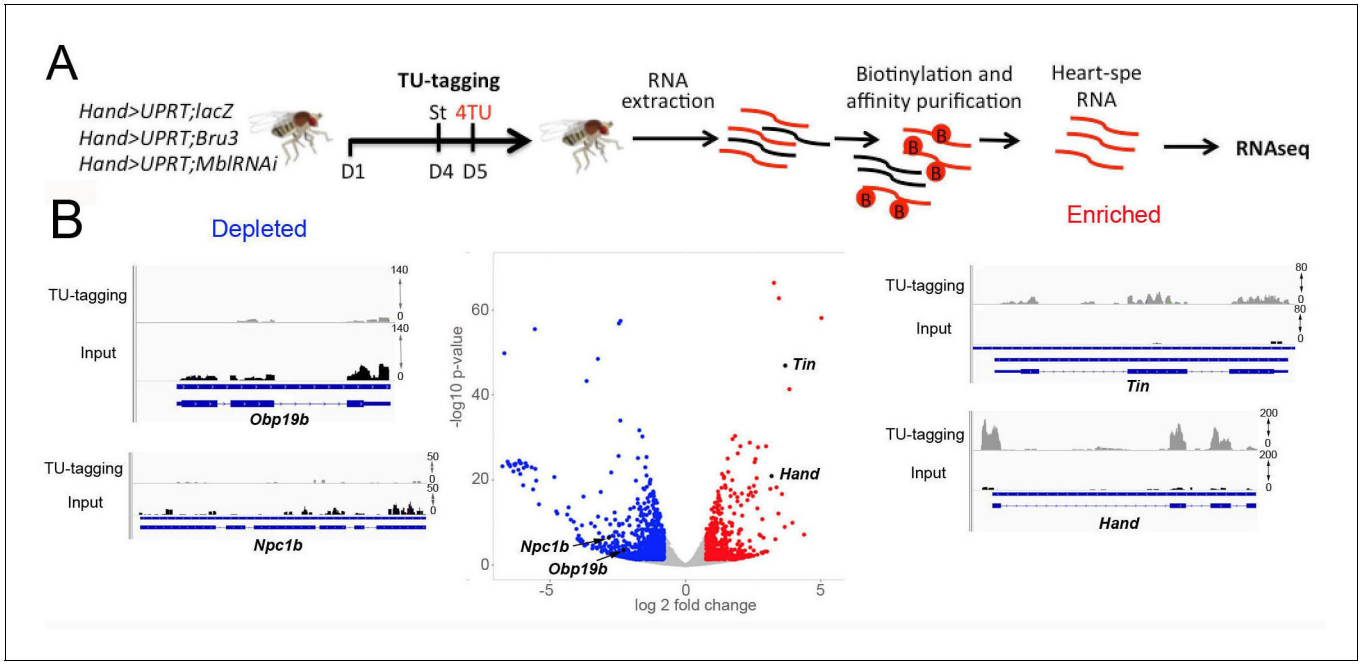

Figure 2. Cardiac-specific transcriptional profiling using TU-tagging method. (**A**) Pipeline of heart-targeted transcriptional profiling using TU-tagging. Note that Gal4- inducible UPRT transgene (*UAS-UPRT*) has been combined with *UAS-MblRNAi* and with *UAS-Bru-3* for the purpose of TU-tagging. *Hand>UPRT;lacZ* is the control line used to identify pathogenic gene deregulations in *Hand>UPRT;MblRNAi* and *Hand>UPRT;Bru-3* contexts. Flies were starved at day 4 for 6 hr before being transferred to 4TU containing food for 12 hr. (**B**) Volcano plot and IGV tracks from control *Hand>UPRT;lacZ* flies show examples of enrichment of heart-specific genes (e.g. *Hand*, *Tin*) (red, right side) and depletion of non-heart-expressed genes (blue, left side), thus validating the specificity of heart targeting.

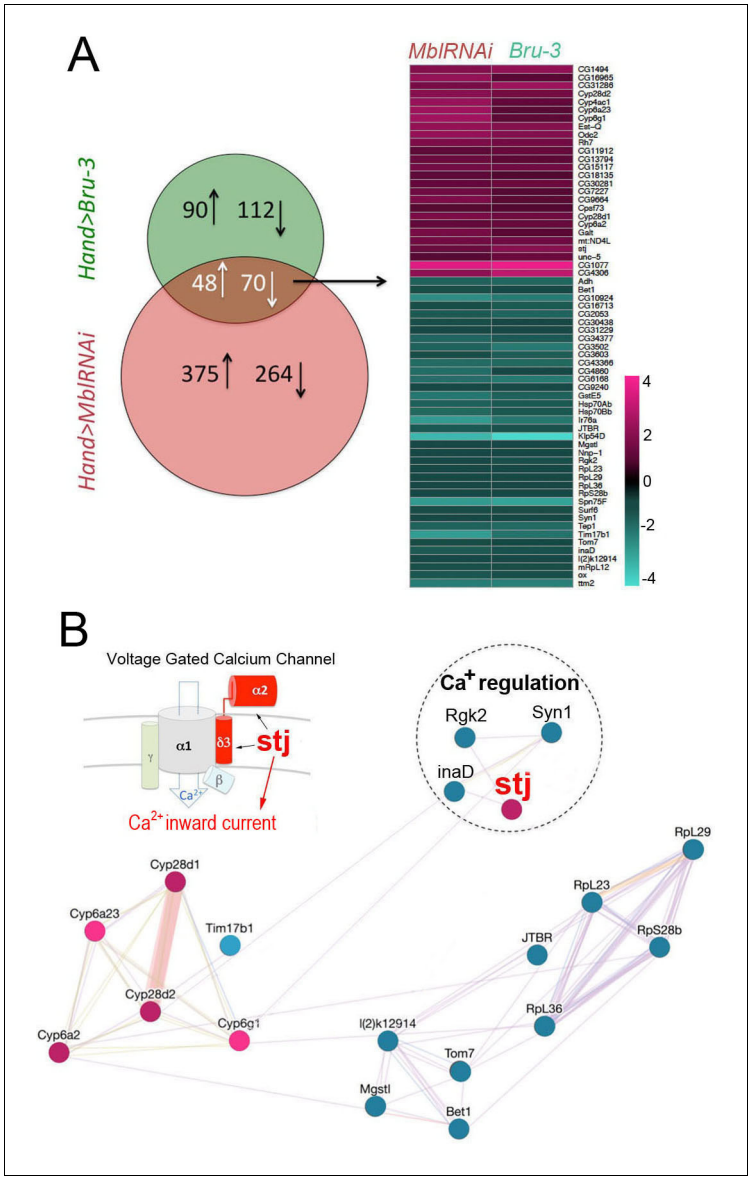

Figure 3. Heart-specific transcriptional profiling of DM1 flies identifies deregulation of genes controlling cellular calcium level. (**A**) Venn diagrams of genes deregulated in *Hand>UPRT;MblRNAi* and in *Hand>UPRT;Bru-3* contexts (FC > 1.7) followed by heatmap of commonly deregulated genes. (**B**) Genemania interaction network of conserved candidates including *stj, Rgk2, Syn1 and inaD* known to be involved in Ca^{2} regulation. A scheme presenting the structure of the voltage-gated calcium channel and its regulatory component Stj/α2δ3 is included. Color code in genemania network represents up and down regulation according to the heatmap. Cyan/Blue intensity code indicates fold change of genes expression in the heatmap.

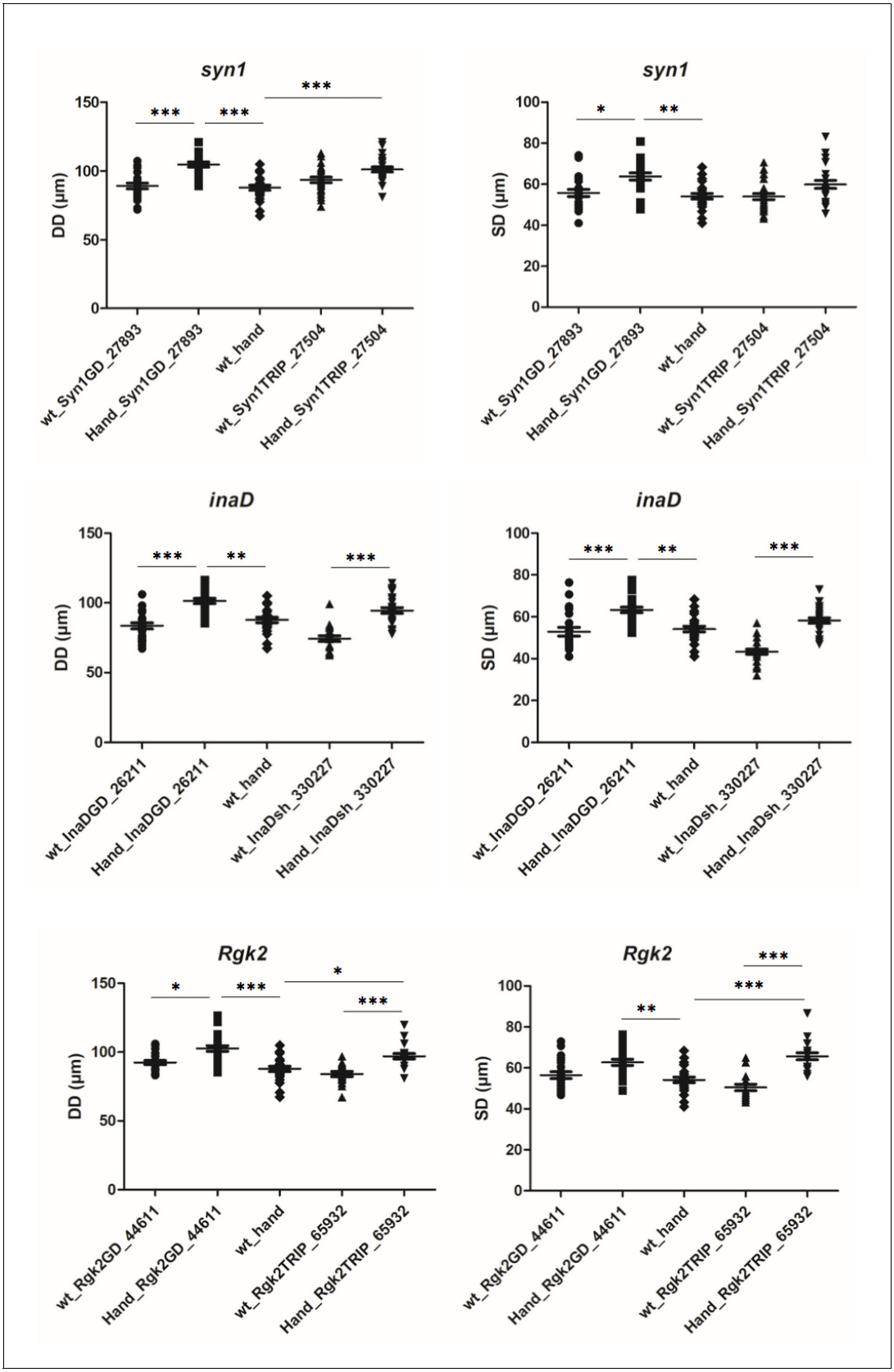

Figure 3—figure supplement 1. Attenuation of *inaD*, *Syn1* and *Rgk2* all lead to an increase of diastolic (DD) and systolic (SD) heart diameters. For each candidate gene effects of attenuation were tested using two different UAS-RNAi lines crossed with Hand-Gal4 driver. More than 20 flies for each

Figure 3—figure supplement 1 continued on next page

Figure 3—figure supplement 1 continued

genotype were analysed by SOHA. Statistical significance of DD and SD changes was assessed using one-way ANOVA, Kruskal-Wallis Dunn's multiple comparison post-test (* - $p<0.05$; ** - $p<0.01$; *** - $p<0.001$).

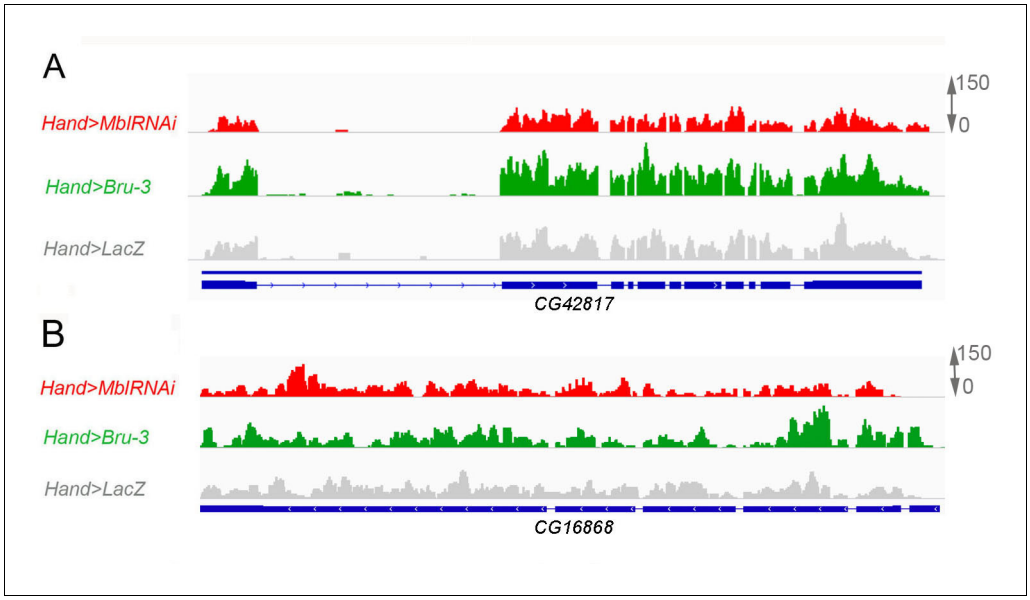

Figure 3—figure supplement 2. The expression levels of *CG42617* and *CG16868*, two additional α2δ protein-coding genes are not affected in the heart of DM1 fly models. Normalized RNAseq IGV tracks in control (*Hand>lacZ*) and in pathogenic DM1 contexts (*Hand>MblRNAi* and *Hand>Bru-3*) are shown aligned with genomic exon/intron organization of *CG42617* (**A**) and *CG16868* (**B**).

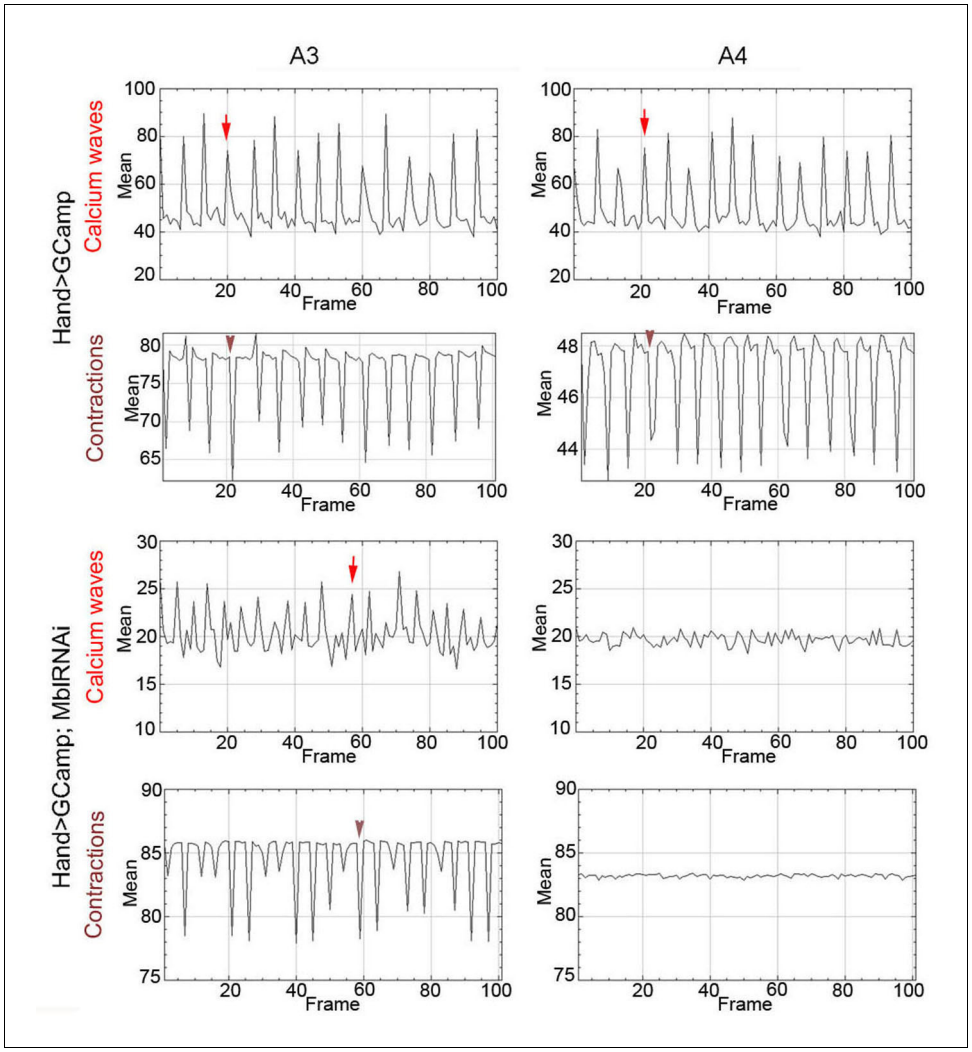

Figure 4. Calcium waves in asynchronous *Drosophila* heart. In wild type hearts, calcium waves underlie cardiac contractions so that calcium peaks (arrows) align with the onset of contractions (arrowheads) in both A3 and A4 segments. In contrast, in asynchronously beating *Hand>MblRNAi* heart, in the anterior A3 segment, calcium peaks (arrows) are not always in perfect alignment with contractions (arrowheads) and could not be detected in A4 segment that does not beat. Notice that GFP signal in *Hand>MblRNAi;GCaMP* context is lower than in the control (*Hand>GCaMP*) most probably because of a lower *Hand-Gal4* induction in two UAS transgene context.

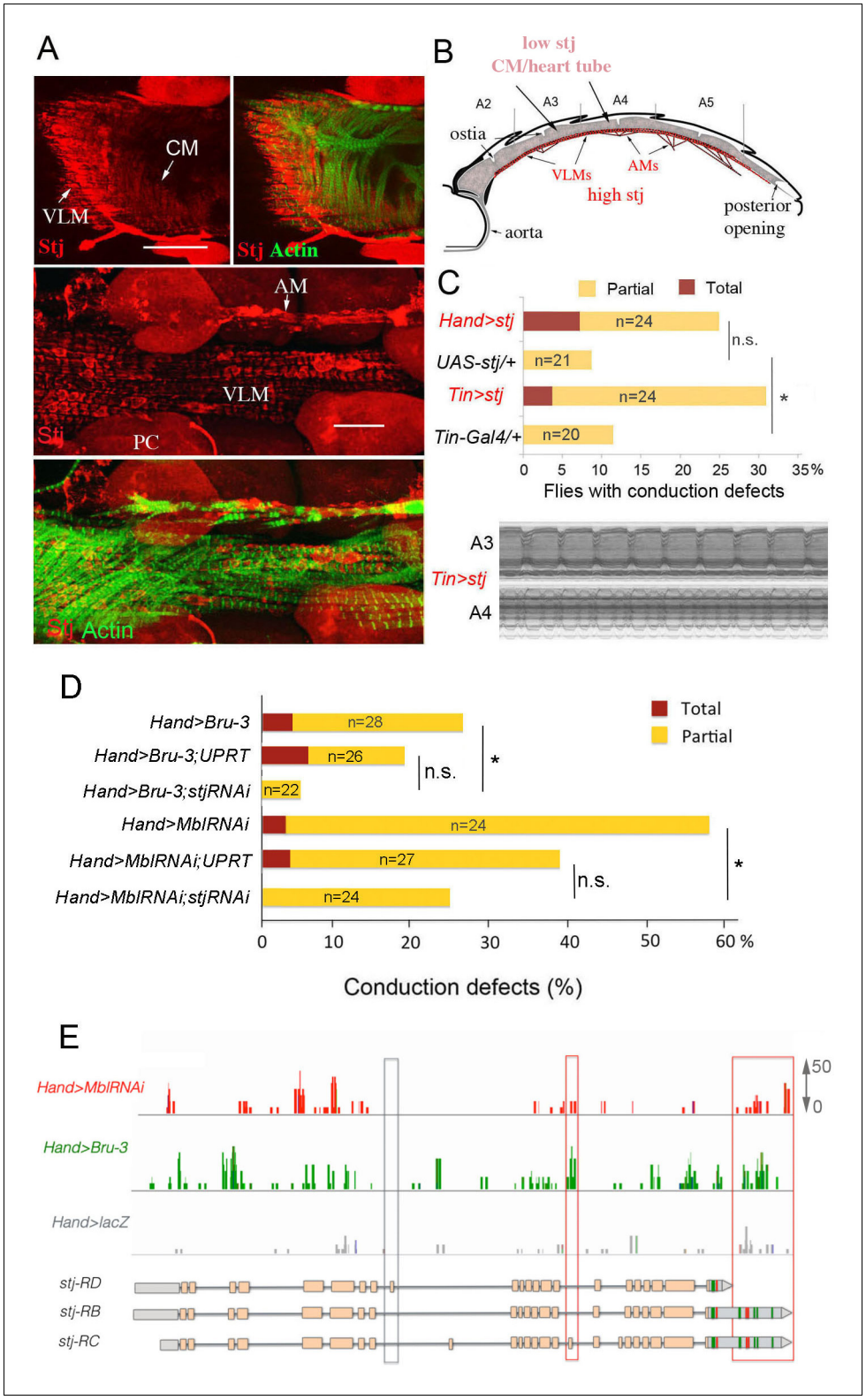

Figure 5. Increased cardiac expression of Stj contributes to the conduction defects observed in DM1 fly models. (**A**) Stj protein is detected at a low level in cardiomyocytes (CM) but at a higher level in the ventral longitudinal muscles (VLMs) that underlie adult heart tube. Stj in VLMs and in heart tube-attaching alary muscles (AMs) marks the network of T-tubules. PC denotes pericardial cells. Scale bars, 50 µm. (**B**) Scheme of the adult *Drosophila* heart with representation of Stj expression. (**C**) Both *Hand-Gal4* (whole heart) and *Tin-Gal4* (cardiomyocytes only) driven

Figure 5 continued on next page

Figure 5 continued

overexpression of *Stj* lead to asynchronous heartbeats similar to those observed in *Hand>MblRNAi* and *Hand>Bru-3* contexts. (**D**) Barplot representing percentage of *Hand>MblRNAi* and *Hand>Bru-3* flies displaying asynchronous heartbeats after reducing cardiac *Stj* expression via RNAi (in *stj* rescue conditions). Notice that lowering Stj expression efficiently reduces the risk of asynchronous heartbeats in *Hand>Bru-3* context. Number of fly hearts tested (n) is indicated and statistical significance (Fisher's exact test) denoted by ns ($p>0.05$) and * ($p<0.05$). (**E**) IGV tracks showing RNAseq peaks over the *stj* locus in healthy control and pathological contexts. Red boxes highlight *stj-RC* – specific exon 15 tracks enriched in *Hand>MblRNAi* and *Hand>Bru-3* contexts and 3'UTR-specific tracks.

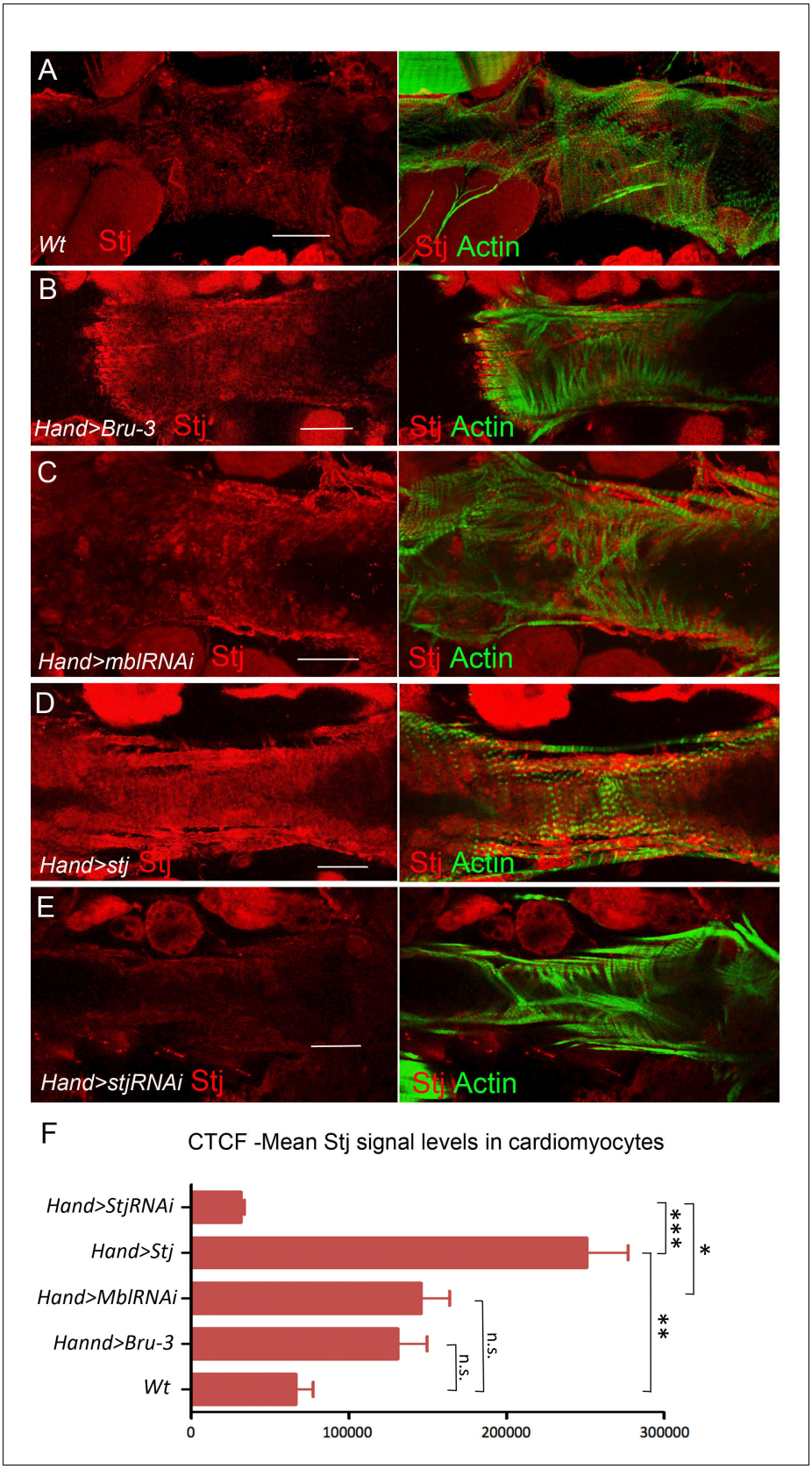

Figure 5—figure supplement 1. Stj protein levels in different genetic contexts visualized by immunostaining. Stj protein expression (red) in circular fibers of cardiomyocytes in wild-type (wt) (**A**) and in different genetic contexts (**B-E**) tested. Circular fibers are visualized with phalloidin staining (green).

Figure 5—figure supplement 1 continued on next page

Figure 5—figure supplement 1 continued

Notice that Stj protein levels appear higher in *Hand>Bru-3* and in *Hand>MblRNAi* compared to wt. High signal level in *Hand>stj* and loss of signal in *Hand>stjRNAi* demonstrate also the specificity of stj antibody. Scale bars, 50 µm. (**F**) Corrected total cell fluorescence (CTCF) of Stj signal in circular fibers of cardiomyocytes (***Figure 5—source data 1***) in different genetic contexts measured using Image J according to ***Burgess et al. (2010)***. Statistical significance (Kruskal-Wallis test) denoted by ns ($p>0.05$) * ($p<0.05$), ** (0.01) and *** ($p<0.001$).

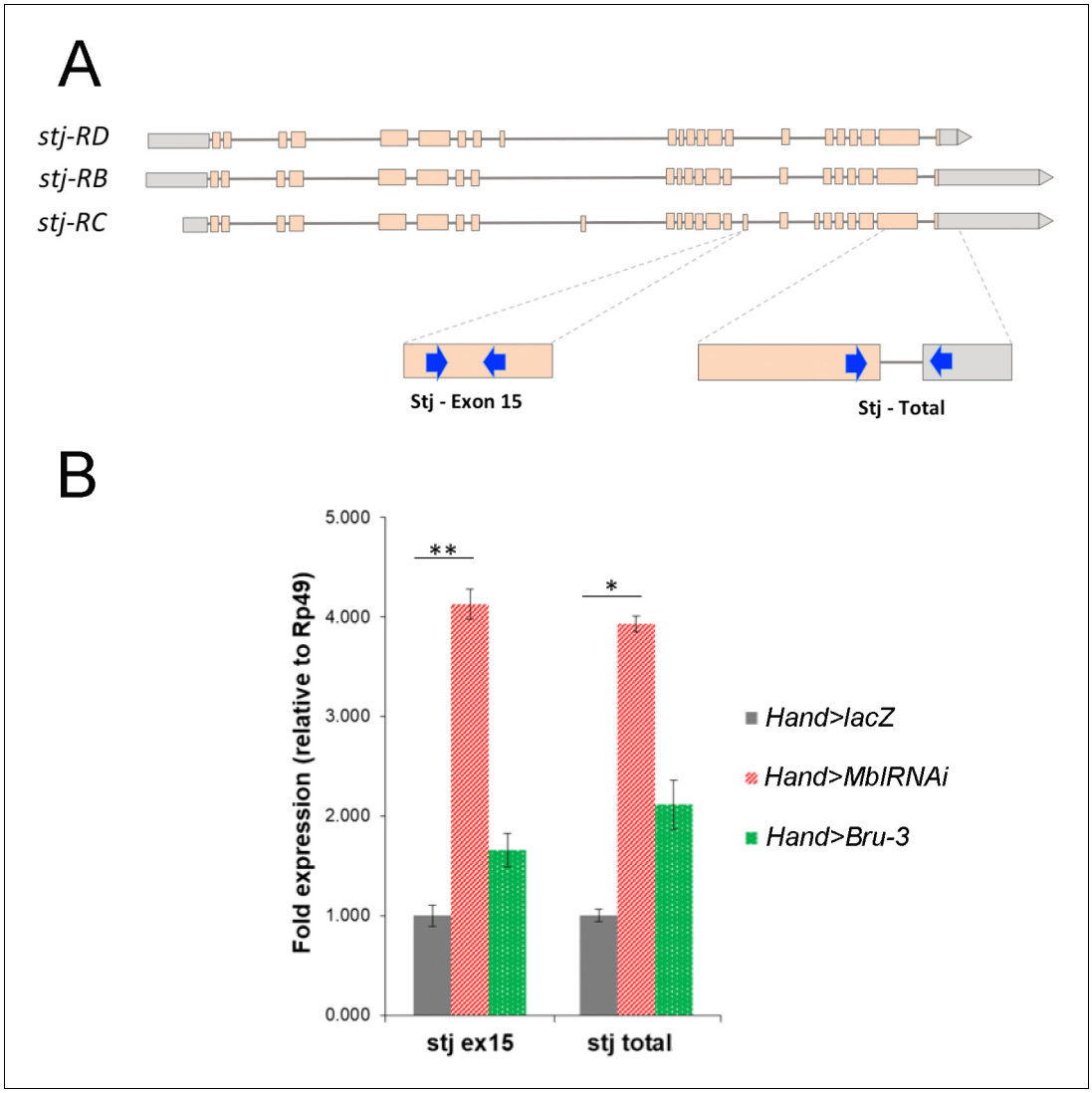

Figure 5—figure supplement 2. *stj-RC* transcript isoform carrying long 3'UTR and alternatively spliced exon 15 is up regulated in *Hand>MblRNAi* and in *Hand>Bru-3* hearts. (**A**) RT-qPCR probes for *stj-RC* specific exon 15 and for total *stj* transcripts are indicated on the scheme. (**B**) RT-qPCR analysis of *stj-RC* and total *stj* transcript levels in control (*Hand>lacZ*) fly hearts and in two DM1 contexts (*Hand>MblRNAi* and *Hand>Bru-3*). One-way ANOVA, Kruskall-wallis Dunn's multiple comparison post-test was applied for assessing statistical significance (* - $p<0.05$; ** - $p<0.001$).

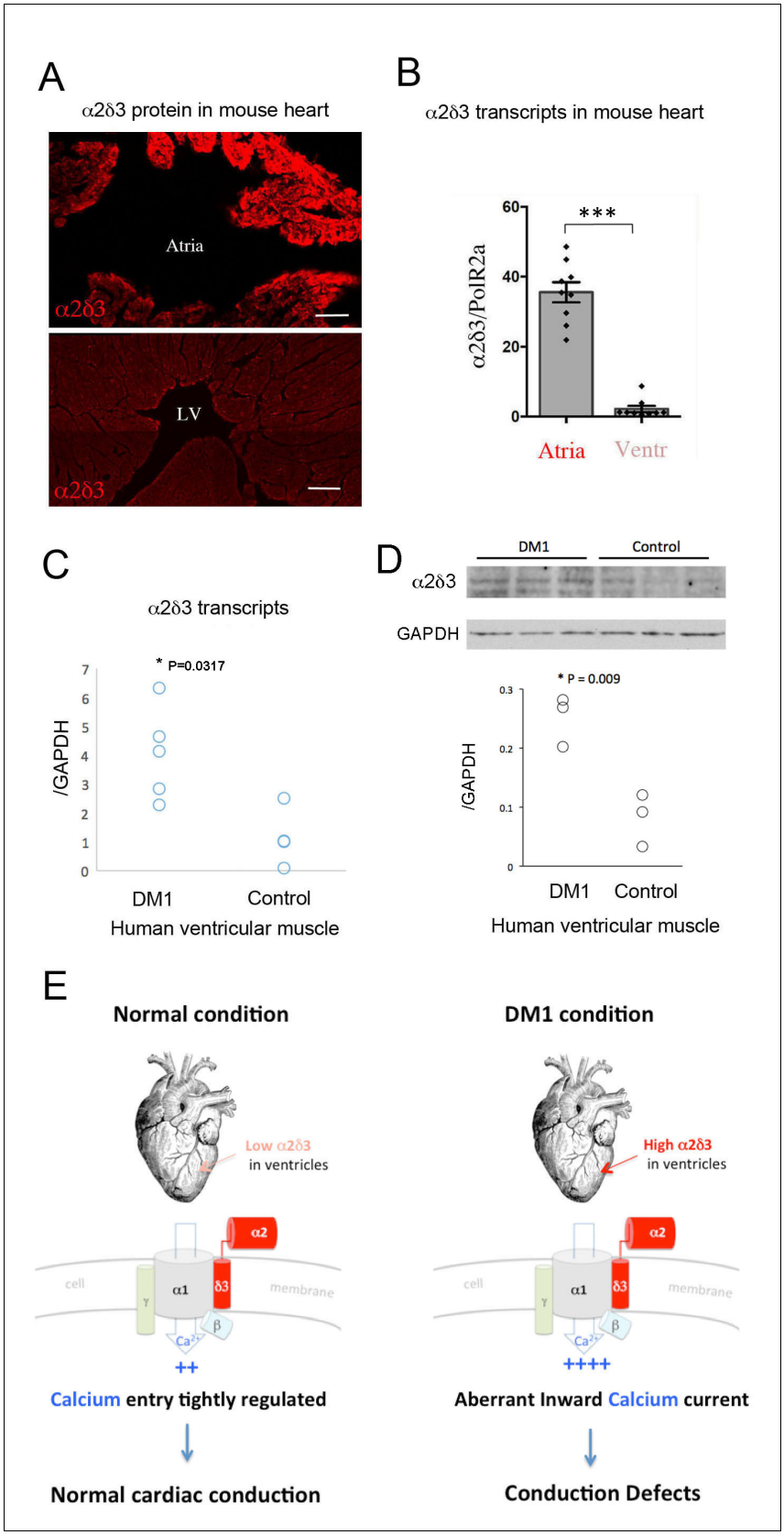

Figure 6. Increased cardiac expression of Straightjacket human ortholog *α2δ3* is associated with conduction defects in DM1 patients. (**A**) In mouse, α2δ3 protein is detected at a high level in atrial cardiac cells and at a low

Figure 6 continued on next page

Figure 6 continued

level in ventricles. LV denotes left ventricle. Scale bars, 100 mm. (**B**) RT-qPCR analysis of mouse α2δ3 transcripts confirms low expression level in ventricles and high expression level in atria. Statistical significance was determined by Mann-Whitney U test (*** $p<0.001$) (**C, D**) α2δ3 (**C**) transcript and (**D**) protein levels analysed by RT-qPCR (**C**) and western blot (**D**) in human ventricular muscle from normal controls and DM1 patients with conduction defects. Note the statistically relevant increase in both α2δ3 transcript and α2δ3 protein levels in ventricles of DM1 patients (Mann-Whitney U test). (**E**) A scheme illustrating normal and DM1 conditions with low and increased α2δ3 levels in ventricular muscle, respectively. In pathological context, the aberrant inward calcium current in ventricular cardiomyocytes could lead to conduction defects and in particular to the IVCD.

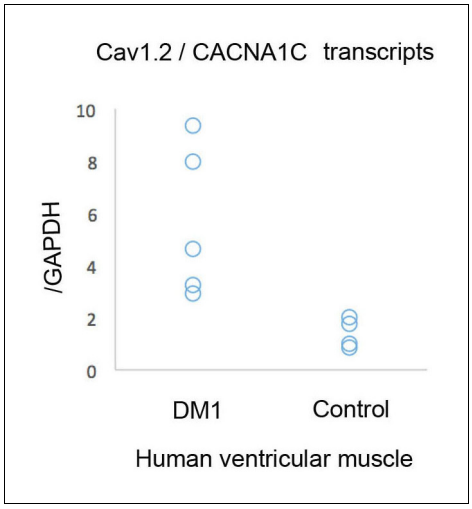

Figure 6—figure supplement 1. RT-qPCR analysis showing that Cav1.2 transcripts are elevated in human cardiac samples from DM1 patients with conduction defects.